Applicability of high-T_c paradigms to magnetic relaxation and irreversibility in superconducting Nb

Matthew F. Schmidt, N. E. Israeloff, and A. M. Goldman
Center for the Science and Application of Superconductivity and School of Physics and Astronomy, University of Minnesota, Minneapolis, Minnesota 55455
(Received 26 January 1993)

Detailed measurements of the temperature and magnetic-field dependence of the magnetization and the magnetic relaxation of Nb films have been carried out. An irreversibility line, below which the remanent magnetization decayed logarithmically in time, was identified. The data were quantitatively compared to predictions of flux-creep, vortex-glass, and vortex-lattice-melting models. Only the melting model self-consistently explained the data.

I. INTRODUCTION

The nature of the magnetic-field–temperature (H-T) phase diagram for high-temperature superconductors has been the subject of intense interest. An irreversibility line and logarithmic decay of the remanent magnetization were first identified by Müller, Takashige, and Bednorz[1] in bulk ceramic La-Sr-Cu-O. They fit their irreversibility line to the form $H \propto (1-t)^{3/2}$, where t is the reduced temperature T/T_c and tentatively identified it as a quasi de Almeida-Thouless line, suggestive of a superconducting glass transition. There has since been an ongoing debate over whether these history-dependent properties are associated with flux creep, a glass transition, or vortex-lattice melting.[2]

The analogy to spin glasses and the suggestion of a superconducting glass transition seemed very reasonable for the ceramic samples of Ref. 1; however, similar magnetic relaxation and irreversibility were later seen in single crystal samples.[3,4] Yeshuran and Malozemoff[4] were able to obtain a $\frac{3}{2}$ power-law irreversibility line using a conventional flux-creep picture. Meanwhile, Tinkham,[5] showed that the flux-creep picture and the superconducting phase-glass model with Josephson-coupled regions of ideal superconducting material are, in fact, closely related. Hagen and Griessen,[6] also working within the context of the flux-creep picture, were able to explain many of the observed time- and history-dependent magnetic properties by invoking a distribution of activation energies. Conflicting results for the dependence of the magnetic relaxation and irreversibility on Pb-ion irradiation[7] and proton irradiation[8] indicate that the detailed nature of the defects and pinning are still not understood. Recent work[9] has extended the conventional flux-creep picture to include complications such as intervortex interactions and thermal fluctuations.

On the other hand, Fisher[10] suggested that in the presence of random pinning sites there exists a disordered phase, the vortex glass, that is truly superconducting. Larkin and Ovchinikov[11] had shown some years ago that the vortex lattice can be destroyed by disorder. Measurements of current-voltage characteristics on high-T_c samples by Koch *et al.*[12] and Gammel, Schneemeyer, and Bishop[13] appear to support the scaling behavior predicted by Fisher, Fisher, and Huse[14] associated with a continuous vortex-glass to vortex-liquid transition. Flux decoration experiments in Bi-Sr-Ca-Cu-O,[15], and certain low-field magnetic memory effects[16] also seem to support a glass picture for disordered type-II superconductors. In the past year, however, some experiments[17] and simulations[18] have suggested that, in the very clean limit, the transition might be first order.

The irreversibility line has also been suggested to be a manifestation of vortex lattice melting.[19] Vortex lattice melting was discussed by Fisher[20] in the context of two-dimensional systems. Houghton, Pelcovits, and Sudbø[19] used a nonlocal elasticity theory and a Lindemann criterion to derive an expression for the melting line in the H-T plane. They found good agreement between their prediction and the irreversibility lines seen in Y-Ba-Cu-O and Bi-Sr-Ca-Cu-O samples. Recent equilibrium torque magnetometry measurements[21] and an observed hysteresis in the current-voltage response of clean, untwinned single crystals of Y-Ba-Cu-O (Ref. 22) both appear to support the melting picture. In addition, Kwok *et al.*[23] identify a "kink" feature in the magnetic-field-broadened resistive transition with melting of the vortex lattice.

Although not necessarily expected,[24] similar irreversibility lines and time-dependent magnetic properties have been observed in conventional type-II superconductors.[25,26] While it is not clear that these features have the same origin as their counterparts in high-T_c materials—which are highly anisotropic and, because of short coherence lengths, more heavily influenced by thermal fluctuations—conventional materials appear to offer a simpler platform for the examination of the consequences of the various models. In this article we present the results of detailed measurements and quantitative analysis of the temperature and magnetic field dependence of the irreversibility and relaxation of Nb. Section II gives an overview of the experimental procedures and results. In Sec. III the data are analyzed in the context of a conventional flux-creep picture and compared to the depinning predictions of Yeshuran and Malozemoff.[4] In Sec. IV,

0163-1829/93/48(5)/3404(13)/$06.00

the scaling approach of Fisher, Fisher, Huse[14] for I-V characteristics is extended to magnetic relaxation measurements using the method of van der Beek,[27] and the data are examined for evidence of a vortex-fluid to vortex-glass transition. The low-temperature magnetic relaxation results are also examined directly for evidence of the vortex-glass phase. In Sec. V, the data are compared to the vortex lattice melting prediction of Houghton, Pelcovits, and Sudbø.[19] It will be seen that the latter comparison gives the best results. Finally, in Sec. VI, we offer a summary and some conclusions.

II. EXPERIMENT

The sample studied in detail was a Nb film prepared by rf sputtering onto an oxide layer of a Si substrate. The film's dimensions were 5000 Å×2 mm×2mm, and its resistivity ratio was 5.9. Field-cooled (FC) and zero-field-cooled (ZFC) magnetization measurements were made in magnetic fields ranging from 100 to 3000 G. These measurements were performed using a Quantum Design superconducting quantum interference device (SQUID) susceptometer with the plane of the sample aligned perpendicular to the direction of the magnetic field. The temperature control parameters of the SQUID susceptometer were adjusted to eliminate temperature overshoot at the sample during the ZFC measurement. To improve the precision of the data, temperature steps were limited to 0.05 K in the region of T^* and T_c, and 16 scans were averaged at each temperature to determine the magnetization. A typical temperature sweep took 12 h. The scan length was limited to 3.0 cm to minimize the effects of moving the sample through a nonuniform field—an experimental problem reported in earlier work using SQUID susceptometers on hysteretic samples.[28,29] The fractional variation in field over this length is less than 0.0005. All results quoted here were found to be scan-length independent for scans less than 4.0 cm. As discussed in Ref. 29, some sample geometries have multiple moments below T^*, making both the ZFC and FC magnetic moment measurements unreliable there; however, the method can still be used reliably to obtain T^* itself. A similar irreversibility line seen in vibrating reed experiments on Nb foils[26]—with the sample held stationary in the solenoid—provides additional evidence that this result is not an artifact of the scanning process.

The zero-field-cooled–field-cooled irreversibility line is determined using a series of temperature sweep experiments conducted in different magnetic fields. The sample starts at a temperature above T_c in zero field; it is cooled through the superconducting transition temperature, and the field is turned on; the magnetic moment is then measured at successively warmer temperatures until the sample is again above T_c; at this point, the temperature sweep is reversed, with the magnetic moment being measured at successively cooler temperatures. Figure 1 shows one such measurement using an applied magnetic field of 1000 G. The mean-field upper critical field $H_{c2}(T)$ is determined by the onset of diamagnetism using the usual intersection of two straight lines method. The irreversibility temperature $T^*(H)$ is, qualitatively, the temperature where the field-cooled (FC) and zero-field-cooled (ZFC) magnetization curves meet. Above T^* the magnetization of the sample was independent of thermal history. Below T^* the ZFC magnetization depended on the direction of the temperature sweep, but the FC magnetization was independent of thermal history. (It has been reported that the FC magnetization of Nb *powder* can be thermal-history dependent,[30] but no evidence of this was seen in this sample.) To improve the precision, several measurements were averaged at each temperature step and $T^*(H)$ was defined as the lowest temperature where the difference between the FC and ZFC magnetizations was less than the standard deviation of the mean of the individual FC and ZFC measurements. The locus of points $T^*(H)$ was identified as the irreversibility line and is shown in Fig. 2.

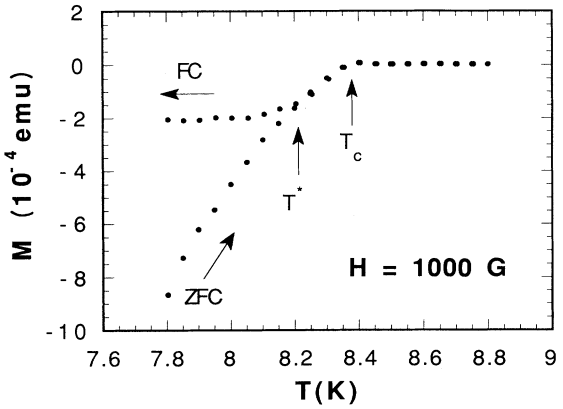

FIG. 1. Zero-field-cooled (ZFC) and field-cooled (FC) measurement of T_c and T^* for $H=1000$ G.

Vanishing of the isothermal magnetic hysteresis has

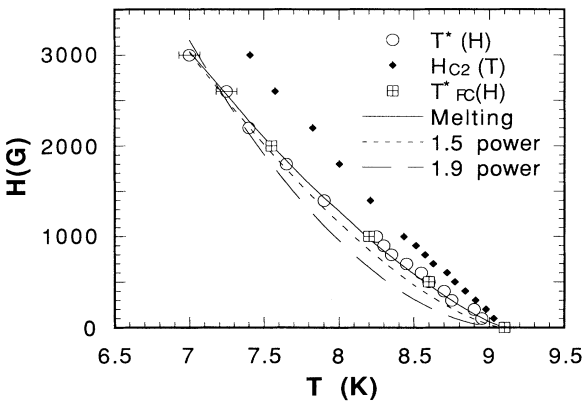

FIG. 2. The H-T phase diagram. The open circles are the ZFC-FC irreversibility temperatures T^*, with uncertainties indicated by the size of the circles (except where error bars are shown explicitly). The solid line is the melting prediction of Ref. 19, and the dashed lines are depinning lines. The squares are $T^*_{FC}(H)$, the temperatures where the FC remanent moment has decreased to the equilibrium value.

also been used to define an irreversibility line.[25,29] It has been reported that this method can give different results than the ZFC-FC method,[25,31] but this was not seen in a limited number of measurements on our sample. Since this method suffers from difficulty in producing the same field during the increasing and decreasing field sweeps due to flux trapping in the superconducting solenoid of the susceptometer,[29] the ZFC-FC method was used for the studies reported here.

The lower critical field $H_{c1}(T)$ can be determined from a plot of magnetization M vs field H, but the procedure is complicated by the high demagnetization factor of the sample.[32,33] Figure 3 shows a typical plot of M vs H. M increases linearly with H at low fields, but the peak is rounded and there is no sharp maximum. M deviates from a linear dependence on field when the flux begins to penetrate at the outer edge of the sample,[33] so this field is defined as H_{c1}. M reaches a maximum at a field $H_{FP}(T)$ when the flux penetration has reached the center of the sample. $H_{c1}(T)$ and $H_{FP}(T)$ are shown in Fig. 4. Defined in this manner, $H_{c1}(T)$ represents a lower bound for the bulk material, and combined with $H_{c2}(T)$ (see Sec. V), gives an upper bound for κ of 10.8.

Measurements of the relaxation of the magnetization after an abrupt change in the applied field are useful for determining the temperature dependence of the activation energy U_0. We performed FC magnetization decay measurements for temperatures from 4.5 to 9.2 K and in fields of 0–2000 G. Typical results are shown in Fig. 5. A magnetic field was applied, while the sample was at $T=15$ K (well above T_c), the sample was then cooled below T_c and T^*, and the field was decreased by $|\Delta H|=1000$ G. The resulting remanent magnetization was found to decay logarithmically on time scales of up to a few hours. The normalized logarithmic decay rates S vs temperature for final fields of 0, 500, 1000, and 2000 G are shown in Fig. 6. The decay rates were normalized to the magnetization measured 10 min after setting the final field to avoid introducing transient effects due to the magnet itself. Comparison with the full-penetration field

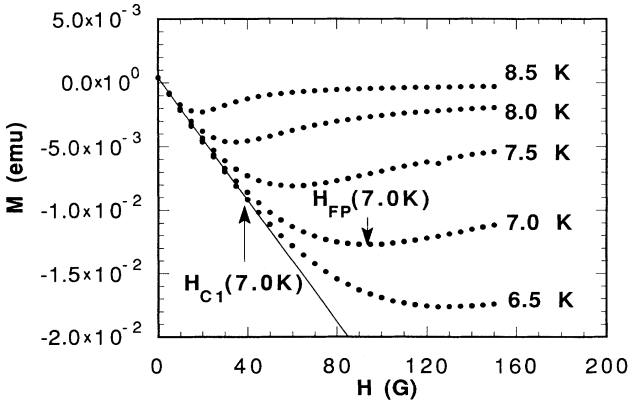

FIG. 3. Magnetization vs field for five temperatures. The lower critical field (H_{c1}) and full penetration field (H_{FP}) are indicated for $T=7.0$ K.

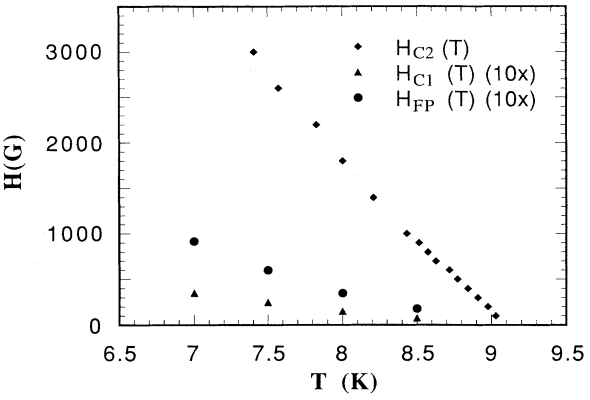

FIG. 4. The upper and lower critical fields in the H-T plane. Note: The lower critical field (H_{c1}) and full penetration field (H_{FP}) have been scaled by a factor of 10 for improved visibility.

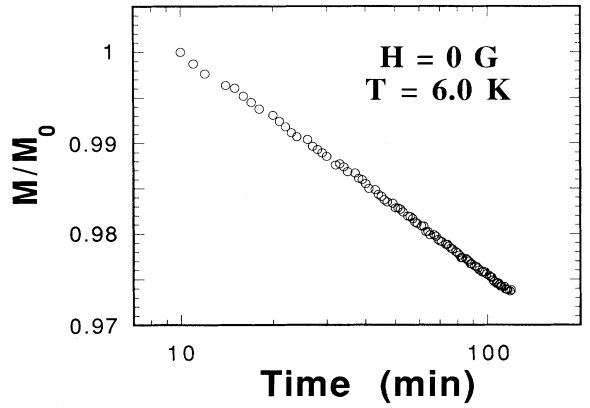

FIG. 5. A typical logarithmic decay of the normalized remanent moment M/M_0 for a final field $H=0$ G at $T=6.0$ K.

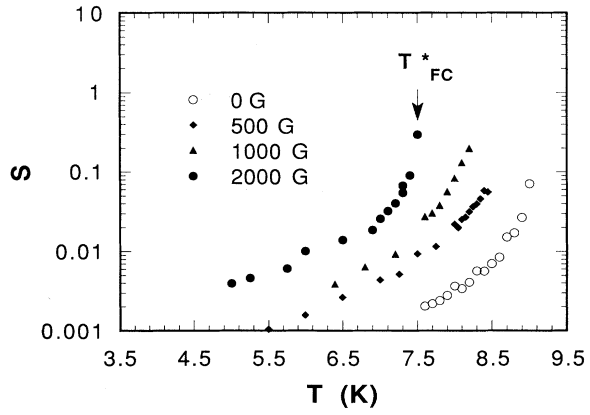

FIG. 6. Normalized logarithmic decay rate S vs temperature. The decay rates were normalized to the remanent moment M_0 measured 10 min after changing the field. Above $T^*_{FC}(H)$ the initial remanent moment has decreased to the FC equilibrium value and no decay is observed.

$H_{FP}(T)$ shown in Fig. 4, shows that $|\Delta H|=1000$ G ensures the entire sample is in the critical state. This is important because a partial critical state would complicate interpretation of the results.[34]

The decay rates shown in Fig. 6 all increase monotonically up to a temperature $T^*_{FC}(H)$, somewhat less than $T_c(H)$, at which point the initial remanent moment has decreased to the field-cooled (FC) equilibrium value—which is very small compared to remanent moments at lower temperatures—and no decay can be discerned. This is in contrast to the results for high-T_c materials, where a peak in the decay rate vs temperature was observed.[6] In Ref. 6, Hagen and Griessen explain this peak within the flux-creep picture by introducing a distribution of activation energies. The absence of a peak in our data suggests a single-activation-energy model would be adequate. The four $T^*_{FC}(H)$ values have also been plotted in the H-T plane of Fig. 2. They are in excellent agreement with the ZFC-FC irreversibility line, which is to be expected if the ZFC-FC and isothermal-hysteresis irreversibility lines are to be coincident.

III. CONVENTIONAL FLUX CREEP AND DEPINNING

In an ideal type-II superconductor (with no pinning), an applied current will produce a Lorentz force on the Abrikosov vortex lattice, leading to flux flow. This will lead to a finite resistance for any applied current. Real type-II superconductors, however, have defects, which cause a local decrease in the superconducting order parameter and the condensation energy, $H_c^2/8\pi$. A vortex, which removes an amount of superconducting condensation energy approximately equal to $(H_c^2/8\pi)(\xi^2 l)$, where l is the vortex length, will thus remove less condensation energy by residing on the defect, which is then a pinning site. Bean[35] developed the "critical-state" model to describe the magnetization of a type-II superconductor with pinning. This model assumes a pinning force which is uniform throughout the sample, and the critical current is the current at which the Lorentz force on the vortices is just large enough to overcome the pinning barrier U_0. The logarithmic relaxation of the magnetization was explained by Anderson and Kim[36] by extending the Bean critical-state model to include thermal activation. (For a more detailed discussion of flux flow, pinning, creep, etc., see Ref. 37).

Yeshuran Malozemoff[4] (YM) suggested the irreversibility line is caused by thermally activated depinning of the vortices. They derived the power-law irreversibility line

$$H \propto \left[1-\frac{T^*(H)}{T_c}\right]^{3/2}, \tag{3.1}$$

where T_c is the zero-field transition temperature. To arrive at this, they assumed that the activation energy scales as $U_0 \propto H_c^2 a_0^2 \xi$, where $a_0=1.075(\Phi_0/B)^{1/2}$ is the flux lattice spacing. The standard Ginzburg-Landau results $H_c \propto (1-t)$ and $\xi \propto (1-t)^{-1/2}$, then led them to

$$U_0(T)=U_0(0)\frac{(1-t)^{3/2}}{B}, \tag{3.2}$$

where $t=T/T_c$. [In the Anderson-Kim theory,[36] U_0 is assumed to scale as $H_c^2\xi^3$, which leads to $U_0 \propto (1-t)^{1/2}$.] By combining Eq. (3.2) with the thermal-activation-dependent critical current,

$$J_c=J_{c0}\left[1-\frac{k_B T}{U_0(T)}\ln\left[\frac{Bd\Omega}{E_c}\right]\right] \tag{3.3}$$

from Ref. 38, and requiring that the critical current be zero, they obtained Eq. (3.1). In Eq. (3.3) J_{c0} is the critical current in the absence of thermal activation, B the magnetic induction, d a distance between pinning centers, Ω an oscillation frequency of a flux line in a pinning well, and E_c a minimum measurement voltage per meter. The logarithm is typically about 30,[4,38] and is considered constant for the purposes of their derivation.

Figure 2 shows the measured irreversibility line and the best-fit $\frac{3}{2}$ power law. The de Almeida–Thouless spin-glass model[39] suggested in Ref. 1 predicts the same $\frac{3}{2}$ power dependence. While at first glance the $\frac{3}{2}$ power-law curve looks reasonable, upon closer examination, it can be seen that it is not as close of a fit to the data as it might be, particularly at the lower fields. The vortex lattice melting curve which is also shown in Fig. 2—and discussed in detail in Sec. V—clearly provides a better fit.

The temperature dependence of the activation energy suggested by Eq. (3.2) is crucial to the derivation of the $\frac{3}{2}$ power-law depinning line of Eq. (3.1). It can be independently checked using remanent magnetization decay studies. In the single-activation-energy picture, when the decay rate is small compared to the magnetization,

$$S=\frac{-1}{U_0(T)/k_B T-\ln(t_b/\tau_0)} \tag{3.4}$$

can be used to ascertain the temperature dependence of U_0. Here t_b is the normalization time, and $1/\tau_0$ is an attempt frequency for hopping, typically on the order of 10^{10} Hz.[6] We assumed $U_0(T)=U_0(0)(1-t)^m$—which is consistent with both the Anderson-Kim and the YM assumptions—and fit Eq. (3.4) to the data for the four fields. Results are shown in Fig. 7. We found

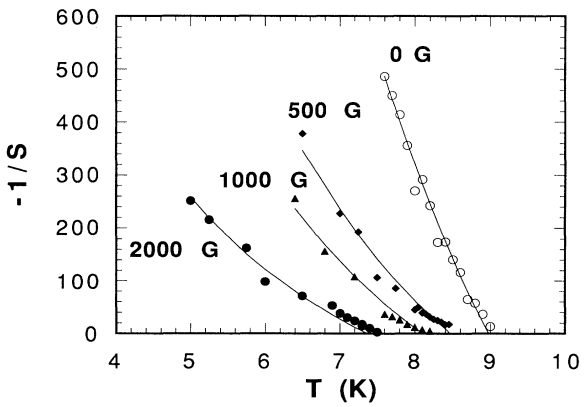

FIG. 7. Inverse logarithmic decay rate $1/S$ vs temperature. The solid lines are results from fitting to Eq. (3.4).

$m = 1.1 \pm 0.1$ for all four fields, which is inconsistent with the YM result $m = 1.5$. When we fit only the higher-temperature data, nearer the irreversibility line, *m decreased,* deviating even farther from the YM prediction.

We also repeated the depinning-line analysis of Ref. 4, but using the temperature dependence of U_0 found from the FC decay data. Where YM assumed the flux bundle volume contained one power of the coherence length ξ, and two powers of the flux lattice spacing a_0, we relaxed the criteria and allowed an unknown power (d) of the coherence length, and assumed $U_0(T)$ scales as $H_c^2 a_0^{3-d} \xi^d$ (this is equivalent to YM when $d = 1$). This led directly to $U_0 \propto (1-t)^{2-d/2}/B^{(3-d)/2}$ and $H \propto (1-t)^{(4-d)/(3-d)}$. In other words, if our irreversibility line was to be the YM depinning line, our FC decay result $U_0(T) \propto (1-t)^{1.1}$ (implying $d \approx 1.8$) suggested we should see $H \propto (1-t)^{1.9}$. This curve is also shown in Fig. 2, with the linear coefficient adjusted to obtain the best fit. It clearly fits worse than the $\frac{3}{2}$ power law. When we reversed the analysis and found the best-fit power law for the irreversibility line, the resulting exponent (1.2) led to the nonsensical result $d = -2$.

On the other hand, pinning defects that extend through the sample thickness (highly plausible given columnar growth of films) suggest a pinning volume given by the sample thickness times the square of the coherence length. This pinning volume, through a similar analysis as above, leads directly to $m = 1$ for the temperature dependence of the activation energy: consistent with the measured magnetic relaxation results below T^*, but still inconsistent with the notion that the irreversibility line is the depinning line. Thus, while the flux-creep picture appears adequate for explaining the magnetic relaxation *below* T^*, the depinning line analysis of Yeshuran and Malozemoff cannot consistently explain the irreversibility line.

IV. VORTEX GLASS

Fisher, Fisher, and Huse[14] (FFH) have considered the effects of thermal fluctuations and quenched disorder on the phase transitions and transport in type-II superconductors in a magnetic field. Fisher[10] first suggested that pinning of vortices due to impurities or other defects (which destroy the long-range spatial correlations of the Abrikosov vortex lattice[11]) combined with other intervortex collective effects, might give a new thermodynamic phase with spin-glass-like off-diagonal long-range order: the *vortex glass.* In contrast to a conventional flux-creep picture, the vortex glass represents a truly superconducting phase with vanishing dc resistance.

According to this theory, fluctuation effects are usually small in conventional type-II superconductors because the characteristic length for fluctuation effects

$$\Lambda_T = \frac{\phi_0^2}{16\pi^2 k_B T} , \tag{4.1}$$

is much larger than any other characteristic length of the system, except very near T_c. Here $\phi_0 = hc/2e$ is the superconducting flux quantum. In the high-T_c materials, higher temperatures, shorter coherence lengths, larger magnetic penetration depths, and quasi-two-dimensionality combine to enhance the effects of thermal fluctuations. Even though these fluctuation effects are expected to be smaller for Nb, they may in fact be apparent under careful analysis. In this section we examine our magnetic relaxation data in the context of FFH, and look carefully for evidence of a vortex-glass phase.

According to FFH, the continuous (second-order) vortex-glass to vortex-fluid phase transition should exhibit a characteristic signature in the *I-V* characteristics. Near the transition, physical quantities are expected to scale with appropriate powers of the vortex-glass correlation length ξ_G and a relaxation time $\tau_G \propto \xi_G^z$, where z is the critical exponent for time. As the transition is approached, the correlation length diverges as $\xi_G \propto |1 - T/T_G|^{-\nu}$, where ν is the critical exponent for the correlation length and T_G is the glass transition temperature. (Note: ξ_G, the glass correlation length, is not the same as the Ginzburg-Landau coherence length, but for simplicity, the subscript will be omitted where there is no likelihood of confusion.) FFH assumed isotropic scaling in D dimensions, which implies that the electric field E scales as 1/(length × time) and the current density J scales as (length)$^{1-D}$. This in turn suggested the scaling form

$$E \xi^{z+1} \approx \tilde{E}_{\pm}(J \xi^{D-1}) , \tag{4.2}$$

for temperatures above (+) and below (−) T_G, with $\tilde{E}_{\pm}$ an appropriate universal scaling function.

In fact, Koch *et al.*[12] provided experimental evidence for just such a continuous phase transition between a vortex glass and a vortex fluid in epitaxial Y-Ba-Cu-O films by demonstrating scaling behavior in the *I-V* characteristics. They used the scaling form

$$E(J) \propto J \xi^{D-2-z} \tilde{E}_{\pm} \left[\frac{J \xi^{D-1} \phi_0}{c k_B T} \right] , \tag{4.3}$$

which is equivalent to Eq. (4.2), and found that their extracted critical exponents were consistent with values expected for the transition from a vortex fluid to a vortex glass. Similar scaling behavior of the *I-V* characteristics has also been seen in numerical simulations.[40] Coppersmith, Inui, and Littlewood[41] have asserted that the scaling behavior demonstrated by Koch and co-workers does not conclusively prove the existence of a vortex glass phase. They suggested that the observed scaling behavior can be explained by assuming an empirical form for the temperature dependence of the activation energy, and then using a conventional flux creep model; however, their model is unable to account for the observed universality of the critical exponents and scaling functions.[42]

van der Beek[27] suggested that the scaling form (4.2) or (4.3) can be used to interpret magnetic relaxation experiments. By calculating the time derivative of the magnetic moment averaged over the sample volume

$$\mathbf{M} = \frac{1}{2cV} \oint_{\text{sample}} \mathbf{r} \times \mathbf{j} \, d^3\mathbf{r} , \tag{4.4}$$

assuming a square platelet geometry, and using Maxwell's equations, he found the magnetic relaxation is

related to the electric field E_S at the sample surface by

$$\frac{\partial M}{\partial t}=\frac{aE_S}{6\Lambda c} , \tag{4.5}$$

where a is the sample edge length, and Λ is the sample self-inductance. The self-inductance accounts for the demagnetization effects on the sample and is given by $\Lambda=\pi a(0.21d+0.03a)/c^2$ in Gaussian units, where d is the sample thickness. Assuming the entire sample has a uniform current density—which is roughly true when the entire sample is in the critical state—he found that the current density at the surface is related to the magnetization by

$$M=\frac{j_S a}{6c} . \tag{4.6}$$

He thus suggests the scaling form

$$\frac{\partial M}{\partial t}\left[\frac{|T-T_G|}{T_G}\right]^{-\nu(z-1)}\approx\tilde{E}_{\pm}\left[M\left[\frac{|T-T_G|}{T_G}\right]^{\nu(1-D)}\right] , \tag{4.7}$$

in analogy to Eq. (4.2).

Using Eq. (4.7), van der Beek demonstrates scaling behavior in the magnetic relaxation data of several Bi-Sr-Ca-Cu-O crystal platelets and finds good agreement between his extracted critical exponents and scaling functions and that of Koch and co-workers. (Although his plot of the collapsed data[43] is not nearly as convincing as that of Koch *et al.*[12])

We looked for evidence of a vortex-glass transition in our Nb film by using van der Beek's relationships between the magnetization data and I-V characteristics. In the argument of the scaling function in Eq. (4.3), the current has been scaled by a characteristic current

$$J_0=\frac{ck_BT}{\phi_0\xi^{D-1}} . \tag{4.8}$$

This can be interpreted as the current at which the free energy of a vortex loop of area ξ^{D-1} perpendicular to the current is equal to the thermal energy k_BT.[14] In Eq. (4.3), the argument of the scaling function includes the k_BT dependence; outside the scaling function, however, the power of ξ has been appropriately scaled, but the k_BT dependence has been neglected. In the scaling analyses of the high-T_c materials, the fractional temperature variation is substantially smaller than it is for our Nb sample, so this is not important. Including the k_BT dependence leaves the slightly modified I-V scaling function

$$E(J)\propto\frac{J}{T}\xi^{D-2-z}\tilde{E}_{\pm}\left[\frac{J\xi^{D-1}\phi_0}{k_BT}\right] . \tag{4.9}$$

Using $\xi\propto|1-T/T_G|^{-\nu}$, $D=3$, and Eqs. (4.5) and (4.6) then leads immediately to

$$aT|1-T/T_G|^{-\nu(z-1)}\frac{1}{M}\frac{\partial M}{\partial t}=\tilde{E}_{\pm}\left[\frac{b|1-T/T_G|^{-2\nu}}{T}M\right] , \tag{4.10}$$

where $M=M(t,T,H)$ is the decaying remanent magnetic moment: a function of time, temperature, and field. Equation (4.10) is the starting point of our scaling analysis.

The goal of the scaling analysis is to find values of ν and z that collapse the magnetic relaxation curves for different temperatures and fields onto two universal curves, one for temperatures above T_G, and one for temperatures below. In principle, T_G, too, is unknown; however, here we will only consider if the ZFC-FC irreversibility line represents a vortex glass transition, not if there is evidence of a transition at some other field-temperature line. With a few complications, the general approach is as follows: First, let

$$x(t)\equiv\ln[M(t)] \tag{4.11}$$

and

$$y(t)\equiv\ln\left[\left|\frac{1}{M(t)}\frac{\partial M(t)}{\partial t}\right|\right] . \tag{4.12}$$

Next, plot $y(t)$ vs $x(t)$ for each of the magnetic relaxation experiments. Since all the relaxation data lie below the irreversibility line, the collapsed data will only show one side of the universal scaling function; the highest temperature data will be closest to, but below, the hypothesized T_G. The prescription will be to shift each curve until they have all collapsed onto the single universal curve for $T<T_G$. With the shifts Δx and Δy thus determined for each curve, we then determine ν and z by requiring

$$\ln\left[\frac{b|1-T/T_G|^{-2\nu}}{T}M\right]=\ln(M)-\Delta x(T,H) \tag{4.13}$$

and

$$\ln\left[aT|1-T/T_G|^{-\nu(z-1)}\left|\frac{1}{M}\frac{\partial M}{\partial t}\right|\right]=\ln\left[\left|\frac{1}{M}\frac{\partial M}{\partial t}\right|\right]-\Delta y(T,H) . \tag{4.14}$$

Equations (4.13) and (4.14) can be immediately simplified:

$$\Delta x(T,H)=2\nu\ln|1-t|-\ln(b)+\ln(T) \tag{4.15}$$

and

$$\Delta y(T,H)=\nu(z-1)\ln|1-t|-\ln(a)-\ln(T) . \tag{4.16}$$

Thus ν and z, and the parameters a and b can be determined using a least-squares curve fit of Eqs. (4.15) and (4.16) to plots of Δx vs T and Δy vs T, respectively. In fact, the plots of Δx vs T and Δy vs T determine if the scaling analysis will be successful: If ν and z, and the parameters a and b can be found so that Eqs. (4.15) and (4.16) match the shifts that were required to collapse the data, then the data can be made to scale with the form (4.10).

As was previously alluded to, there are some complications: First, for typical relaxation experiments, the remanent moment relaxes very slowly, decreasing by only

a few percent over several hours. On the other hand, a small change in temperature produces a comparatively large change in the remanent moment. Thus, over most of the temperature range, the y-vs-x curves for adjacent temperatures do not overlap, making it difficult to unambiguously determine the shifts Δx and Δy. This is not so much due to temperature steps that were too large, but rather the asymmetry in relaxation in time and temperature. Another problem is that noise in the relaxation data—which is most prominent when the remanent moment is smallest, nearest T_G—is magnified in the process of numerically calculating the discrete derivative $\partial M/\partial t$, contributing additional ambiguity to the shifts. In fact, successively measured magnetic moments often increase—even though the overall trend is decreasing—causing the discrete derivative to be entirely unusable due to the oscillation in sign.

Both of these difficulties can be overcome by fitting the relaxation data to some appropriate function, and using smoothed data from the fitting function—extrapolated in time so the y-vs-x curves from adjacent temperatures overlap—to determine Δx and Δy unambiguously. One choice for the fitting function is the logarithmic decay equation

$$M(t)=M_\tau - r\ln(t/\tau)\ . \tag{4.17}$$

Here τ is the normalization time (10 min), M_τ is the remanent moment at time τ, and $r>0$ is the logarithmic decay rate. Using Eq. (4.17), we can perform the scaling analysis using only the information provided by the initial remanent moment and the logarithmic decay rate. Of course, this assumes that the actual relaxation curves are well represented by Eq. (4.17) and that the relaxation is actually logarithmic out to the times to which we extrapolate in order to obtain an overlap for adjacent temperatures. (This will be discussed again later.)

To illustrate the procedure, a graphical method for obtaining the shifts Δx and Δy is shown below. Figure 8 shows y vs x for four temperatures at $H=500$ G. To emphasize the curvature with increasing time and illustrate the scaling methodology, each curve has been plotted from $t=\tau=10$ min out to $t=10\,000$ min, even though the actual decay experiments typically ended at 100 min. Without the extrapolation, the relaxation data for each temperature would appear to be almost linear, with only a slightly different slope for each different temperature. (If the curves were, in fact, linear with different slopes, the data could not be scaled.) Each relaxation experiment starts at the top of the curve, with increasing time indicated by the open-headed arrow.

Without some objective criteria, determining the shifts would be somewhat arbitrary. To avoid this ambiguity, we required that the collapsed data be both smooth and continuous; i.e., we required the resulting universal scaling function be continuous, and that it have a continuous first derivative. We use Δx to shift each curve to maintain a continuous first derivative and Δy to then obtain a continuous function. This procedure is carried out graphically for each relaxation curve as illustrated in Fig. 8. First, since $T=8.55$ K is the highest temperature, and closest to the hypothetical glass temperature $T_G=8.6$ K at 500 G as determined from the irreversibility line, it becomes the reference temperature $T_{\rm ref}$. Since the next curve $T=8.45$ K has a slightly higher initial slope than the reference curve, we find the time t^* where its slope, which decreases as time increases, just matches the slope of the reference curve at the starting time $t=\tau=10$ min. We then determine Δx by requiring that this point have the same x coordinate as the reference curve has as its starting time; i.e., we require

$$x(T_{\rm ref},\tau)=x(T,t^*)-\Delta x\ . \tag{4.18}$$

Δy is then determined by simply shifting the $T=8.45$ K

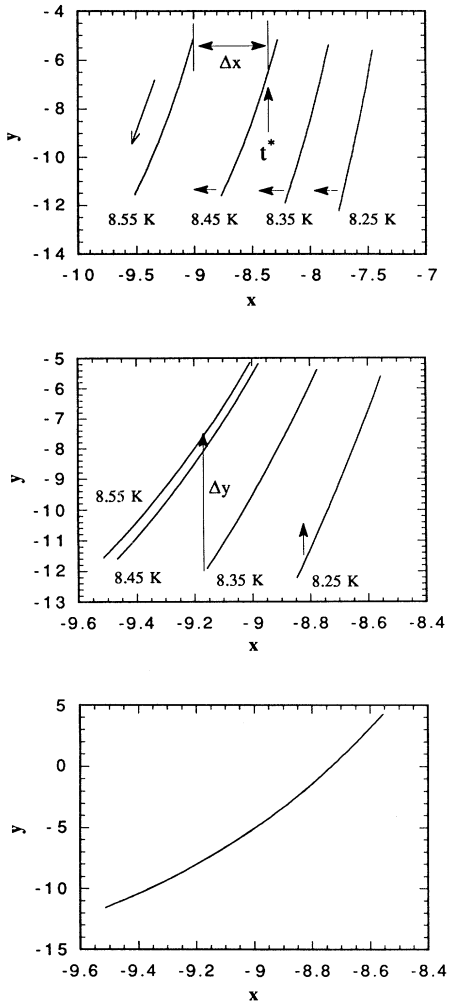

FIG. 8. Graphical illustration of the method used to shift the individual relaxation experiments onto a single curve: the universal scaling function. Relaxation data from four temperatures are shown. The highest temperature, $T=8.55$ K $=T_{\rm REF}$ becomes the reference curve. The next curve, $T=8.45$ K is first shifted horizontally (top figure to middle figure) so its slope matches the reference curve at $t=0$ (increasing time is indicated by the open-head arrow). It is then shifted vertically (middle figure to bottom figure) until it lies directly on top the reference curve. The procedure is then repeated for the next temperature, etc.

curve up, until it lies directly on top of the reference curve. This procedure is then repeated, yielding a Δx and Δy for each temperature, and the universal scaling function shown in Fig. 8.

The graphical method illustrated above can be used for each combination of temperature and field, but Eq. (4.17) offers us an easier, analytical method for calculating Δx and Δy directly. The procedure is the same as the illustration above. Combining Eqs. (4.11), (4.12), and (4.17) immediately yield

$$x(t)=\ln\left[1-\frac{r}{M_\tau}\ln\left[\frac{t}{\tau}\right]\right] \tag{4.19}$$

and

$$y(t)=\ln\left[\frac{r/t}{M_\tau - r\ln(t/\tau)}\right], \tag{4.20}$$

which can be combined to give

$$\frac{dy}{dx}(t)=\frac{dy/dt}{dx/dt}=\frac{M_\tau}{r}-\ln\left[\frac{t}{\tau}\right]-1 . \tag{4.21}$$

Using Eq. (4.21), we determine t^* by requiring

$$\frac{dy}{dx}(T_{\rm ref},\tau)=\frac{dy}{dx}(T,t^*) , \tag{4.22}$$

which gives

$$\ln\left[\frac{t^*}{\tau}\right]=\frac{M_\tau}{r}-\frac{M_\tau^{\rm ref}}{r_{\rm ref}} . \tag{4.23}$$

Finally, using Eq. (4.18) and an identical equation for y, we have the desired results:

$$\Delta x=\ln\left[\frac{r}{r_{\rm ref}}\right] \tag{4.24}$$

and

$$\Delta y=\ln\left[\frac{M_\tau^{\rm ref}}{r_{\rm ref}}-\frac{M_\tau}{r}\right] . \tag{4.25}$$

We are now in a position to see if the data scales: We simply plot Δx and Δy vs T and see if the curves can be fit using (4.15) and (4.16). Figure 9 shows $\Delta x-\ln(T)$ vs $t=T/T_G$ for the four final fields, 0, 500, 1000, and 2000 G. The circles and squares are the values from Eq. (4.24); the thin lines are curve fits of Eq. (4.15) for each individual field; the thick line is a curve fit of Eq. (4.15) on the data from all four fields simultaneously. The results are summarized in Table I. The uncertainty indicates the degree of redundancy in the parameters, i.e., the degree to which one could be traded off against the other without sacrificing the quality of the fit. There is a sizable scatter in the values of ν, which is expected to be universal and independent of field,[14] and, for all fields, ν is substantially less than the value predicted for a vortex glass transition ($\nu=1.7$), and seen in the other experiments.[12,27] In fact, $\ln(b)$ should also be field independent (as will be discussed below); so if the data in Fig. 9 were going to scale, all four curves should have collapsed onto one single curve.

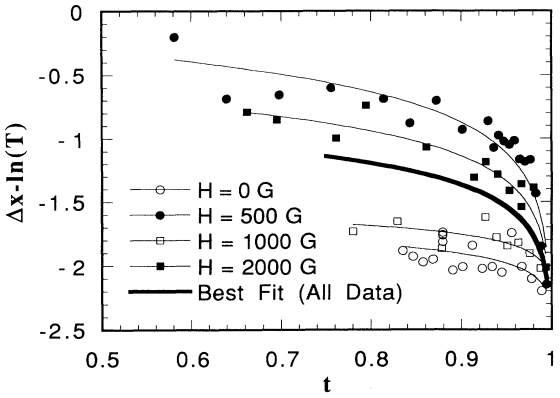

FIG. 9. Scaling results for the four field values. The circles and squares are the results from Eq. (4.24). The thin lines are curve fits of Eq. (4.15) to the individual fields; the thick line is best-fit result from (4.15) when the data from all four fields was fit simultaneously.

Since scaling is only expected in the critical regime near T_G, we also tried restricting the curve fit to the data points nearest T_G. The results of this limited-range curve fitting are summarized in Table II. Not surprisingly, restricting the data to temperatures near T_G improves the fit, but the spread in ν is worse [it is clear from Fig. 9 that ν and $\ln(b)$ are field dependent even near $t=1$], and ν is still substantially smaller than the values typically quoted for a vortex glass.

We can also check the parameter b, to see if it is physically reasonable. Comparing Eqs. (4.10) and (4.9), and using (4.6), we find

$$b=\frac{6\phi_0\xi_0^2}{a^3 dk_B} . \tag{4.26}$$

[The extra factor a^2d = volume is required to relate magnetization in Eq. (4.6) to magnetic moment in Eq. (4.10).] All the quantities are known except ξ_0, the zero-temperature glass correlation length. As mentioned above, the glass correlation length is *not* the same as the Ginzburg-Landau coherence length; however, it is reasonable to expect that the Ginzburg-Landau coherence length, which is related to the core size of an *individual* vortex, represents a lower bound for the vortex glass correlation length, which is a length scale governing collective effects for many vortices. Using $\ln(b)\approx 2$,

TABLE I. Results of fitting Eq. (4.15) to the $\Delta x(T)$ data generated using Eq. (4.24).

H (G)	T_G (K)	ν	$\ln(b)$
0	9.10	0.054±0.018	1.7±0.1
500	8.60	0.17±0.02	0.074±0.089
1000	8.20	0.050±0.016	1.5±0.1
2000	7.55	0.14±0.01	0.48±0.08
All fields		0.12±0.03	0.73±0.17

TABLE II. Results of the restricted-temperature-range curve fit of Eq. (4.15) to the $\Delta x(T)$ data. The data was restricted to the data points nearest T_G, i.e., $T/T_G > 0.95$.

H (G)	T_G (K)	ν	$\ln(b)$
0	9.10	0.15±0.05	0.93±0.38
500	8.60	0.31±0.04	−0.99±0.30
1000	8.20	0.07±0.011	1.4±0.1
2000	7.55	0.16±0.05	0.37±0.39
All fields		0.16±0.05	0.47±0.38

TABLE III. Results of fitting Eq. (4.16) to the $\Delta y(T)$ data from Eq. (4.25) with $T/T_G > 0.95$.

H (G)	T_G (K)	$\nu(z-1)$	$\ln(a)$
0	9.10	−38±3	170±10
500	8.60	−4.5±1.7	19±7
1000	8.20	−17±3	74±9
2000	7.55	−14±3	63±9
All fields		−13±4	60±15

which is a rough upper bound for the results above, yields 2 Å for the zero-temperature glass correlation length. This is much smaller than the Ginzburg-Landau zero-temperature coherence length $\xi_0 = 175$ Å, as determined from the slope of the H_{c2} vs T curve, and thus too small to be physically reasonable. Also, Eq. (4.26) suggests $\ln(b)$ should, like ν, be independent of field, which it clearly is not, adding a further strike against the scaling analysis.

The situation for Δy is even worse. Figure 10 shows Δy vs T for the final field $H = 500$ G over the full temperature range of available data. The data from the other three fields looks similar. Again, the open circles represent the calculated values from Eq. (4.25), while the solid line is the two-parameter fit of Eq. (4.16). It is quite clear that the functional form (4.16) with its positive curvature is not at all representative of the data, which show a distinct negative curvature. Again, the quality of the fit can be improved by restricting to the temperature regime nearest to T_G, but the resultant exponents are entirely unreasonable. Table III summarizes the extracted exponents obtained when the temperature range was restricted to $t = T/T_G > 0.95$. The fits are not particularly close, and the negative sign of the extracted exponents is entirely unreasonable. Using $\nu = 0.16$, from the all-field results of Table II, then suggests $z \approx -80$, as opposed to $z = +4.8$.[12,27]

Clearly, this scaling analysis offers no evidence that the irreversibility line is due to a vortex glass transition. A plot of the scaled data, yielding a universal scaling function in analogy to van der Beek's result,[43] might be constructed for the limited temperature range $t > 0.95$, but it would require using values of ν and z that are not only inconsistent with the values quoted for the vortex glass transition, but are also entirely unphysical; the final result, the universal scaling function, would be similar in form to the collapsed data shown in Fig. 8 that displays positive curvature, inconsistent with the universal scaling function of Koch and van der Beek for $T < T_G$. Actually, close examination of van der Beek's results[43] shows that while his scaling function for $T < T_G$ does display the expected negative curvature, it is pieced together from individual data sets that show positive curvature, indicating he may have encountered this difficulty as well.

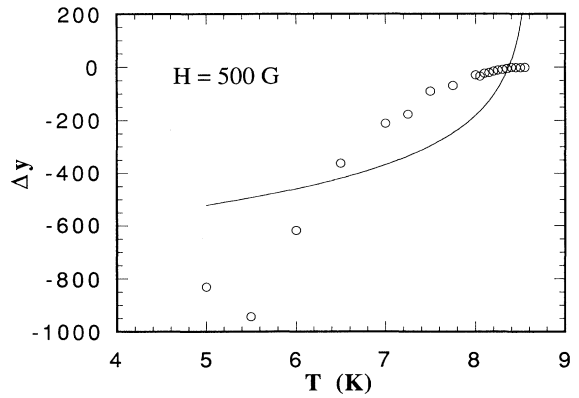

FIG. 10. Scaling results for the $H = 500$ G data from Eq. (4.25). The thin line is a least-squares fit of Eq. (4.16).

One objection that might be raised relates to the validity of using Eq. (4.17) to extrapolate to times well beyond the duration of the actual decay experiments. In fact, it could be argued that use of Eq. (4.17), which arises naturally in a traditional flux-creep picture, is not appropriate for representing the long-time behavior of a vortex glass. To check that the failure of the scaling analysis was not simply a result of having used the flux-creep equation (4.17), the analysis was repeated for the 500-G data but using the vortex-glass prediction[14]

$$M(t) = M_0[\ln(t/t_0)]^{-1/\mu} , \tag{4.27}$$

which is valid for $t \gg t_0$, where t_0 is a microscopic time of order 10^{-9} sec.

The method used for the scaling analysis is entirely similar to that described above. Equation (4.27) was fit to the relaxation data, yielding $M_0(T)$ and $1/\mu(T)$ for each temperature, as shown in Fig. 11. Equations (4.27) and (4.17) fit the data equally well, with no discernible difference in the quality of the fit. Following the analysis of Eqs. (4.19)–(4.25), but using Eq. (4.27) instead of Eq. (4.17) yields

$$\Delta x = \ln\left[\frac{M_0[\ln(\tau/t_0)]^{-1/\mu}}{M_0^{\rm ref}[\ln(t^*/t_0)]^{-1/\mu_{\rm ref}}}\right] \tag{4.28}$$

and

$$\Delta y = \ln\left[\frac{\mu_{\rm ref} t^*}{\mu\tau}\left[\frac{\ln(t^*/t_0)}{\ln(\tau/t_0)}\right]\right] \tag{4.29}$$

with

$$\ln(t^*/t_0) = \frac{\mu}{\mu_{\rm ref}}[\ln(\tau/t_0)+1]-1 . \tag{4.30}$$

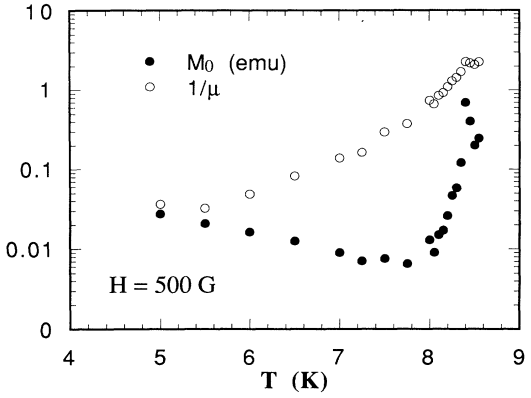

FIG. 11. M_0 and $1/\mu$ vs temperature for the relaxation data with final field $H=500$ G. M_0 and μ were determined by fitting Eq. (4.27) to the data from the individual relaxation experiments.

Figure 12 shows Δx and Δy vs T. When Eq. (4.15) is used to fit the Δx vs T data, ν ranges from 2.1 to 1.1 as the fit is restricted from all the data to $T>8.0$ K. This suggests the result $\nu=1.7$ could be "fudged" by appropriately choosing an intermediate temperature range, but the fit is not very good, and the upper bound $\ln(b)=-8$ suggests the entirely unphysical zero-temperature glass correlation length of 0.01 Å. The situation for Δy has not improved: The data still show positive curvature so fitting to Eq. (4.16) gives similar results as seen in Fig. 10. Restricting the fit to $T>8.2$ K gives the smallest z, but the resulting value ($z\approx 13$) is still too large to be consistent with a vortex-glass transition.

The drastic difference in the resulting exponents obtained from using Eq. (4.27) as opposed to Eq. (4.17) does not bode well for this method: It leaves one wondering if some other, still-untried functional form might give still different results. This is a result of the large extrapolations in time that were used to do the scaling. In order to get accurate results from this sort of scaling analysis, it is

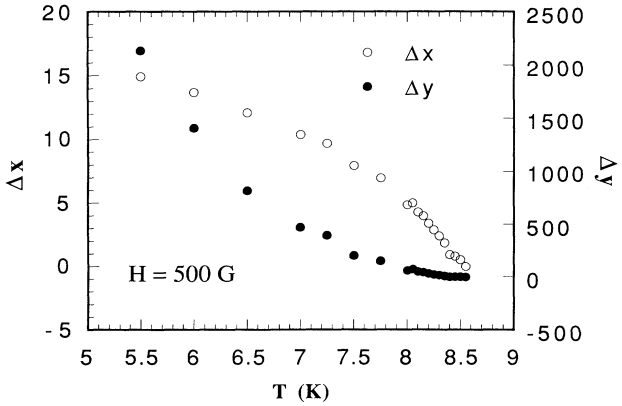

FIG. 12. Scaling results for the $H=500$ G data when Eqs. (4.28) and (4.29) were used to calculate the horizontal and vertical shifts.

necessary for the I-V characteristics to span many orders of magnitude;[42] but in magnetic relaxation experiments, relatively little change in the magnetization (current) is seen in a reasonable experimental time. Because of this, and the additional reasons discussed below, we did not pursue the scaling analysis any farther.

As alluded to, there is also another criticism that might be raised: At these fields the width of the critical regime, the region in which scaling behavior would be expected, is probably too narrow to be observed. Koch *et al.*[12] found that the scaling was not as good and the exponents were not universal when the applied field was less than 1 T. They suggest that the critical regime for the vortex-glass–to–normal phase transition requires that the vortex-glass correlation length ξ be greater than the average distance between flux lines

$$l\approx(\phi_0/\pi H)^{1/2}\ . \tag{4.31}$$

We note the average vortex spacing given by Eq. (4.31) is slightly less than the spacing in a vortex *lattice* discussed in Secs. III and V. When $T<T_G$, the characteristic current density J_0 given by (4.8) is essentially the critical current density of the superconducting phase,[12] so we can obtain a rough estimate of ξ by combining Eqs. (4.6) and (4.8). If the entire sample is in the critical state, the surface current density j_S in Eq. (4.6) should equal the critical current density. The requirement $\xi>l$ recast in this matter yields

$$M(t,T,H)<\frac{(\pi a^3 d)Hk_BT}{6\phi_0^2}=(7.2\times10^{-10})HT\ . \tag{4.32}$$

This, albeit crude, criterion suggests that at the highest field we measured, 2000 G, the remanent moment must be less than 1.1×10^{-5} emu for scaling behavior to be expected. In fact, the measured remanent moment is larger than this even at the highest temperatures measured. At the lower fields the criterion is even more restrictive with the width of the critical regime finally decreasing to zero in zero field.

In summary, because of the limited range of currents probed, we can probably conclude that magnetic relaxation experiments are not likely to be a useful probe in looking for scaling evidence of a vortex-fluid–to–vortex-glass transition. In the final analysis we are left with a somewhat disappointing conclusion: While the scaling analysis offers no evidence the irreversibility line *is* due to a vortex-glass–to–vortex-fluid phase transition, neither does it entirely eliminate the possibility.

Not discouraged, we can still, however, examine the low temperature data for any direct evidence of the vortex-glass phase. Equation (4.27) arises in both vortex-glass theory[14] and collective flux-creep theory.[44] Both theories suggest dissipation is caused by jumps of vortex-bundle segments, forming vortex loops of a characteristic length scale, but the two theories approach it from opposite extremes:[45] vortex-glass theory from long-length scales, and collective creep from short-length scales. Both theories suggest a nonlinear dissipative electric field

$$E(J)\propto\exp[-(J_T/J)^{\mu}] \tag{4.33}$$

(J_T is a characteristic current for the onset of thermally activated dissipation), which leads to an extremely slow relaxation of a persistent current or remanent magnetization.

The origin of Eq. (4.27) can be explained as follows:[14] After an abrupt change in field, the nonequilibrium current distribution first relaxes via deterministic phase slip to the critical current density for nonactivated dissipation J_F on a microscopic timescale ($t < t_0 \leq 10^{-9}$ sec). After this, the current decays via thermally activated nucleation of vortex loops at a rate $\partial J/\partial t \propto E(J)$, with $E(J)$ given by Eq. (4.33). Integrating with respect to time gives the long-time decay form (4.27) [assuming $M(t) \propto J(t)$]. Nattermann[46] suggests an interpolation formula for times that are longer than microscopic ($t \gg t_0$) but not yet in the long-time limit:

$$J(t) \approx \frac{J_F}{[1+(k_B T/U)\ln(t/t_0)]^{1/\mu}} \tag{4.34}$$

with

$$U/k_B T \approx (J_T/J_F)^{\mu} . \tag{4.35}$$

The crossover time t_{cr}, which separates the regimes of Eqs. (4.27) and (4.34), is given by

$$t_{cr} = t_0 \exp(U/k_B T) . \tag{4.36}$$

[Interestingly, for times greater than microscopic, but still much less than t_{cr}, Eq. (4.34) reduces to the same form as the standard flux creep result Eq. (4.17).]

We can determine which time regime is appropriate by determining the barrier height U. We use the result for the normalized logarithmic decay rate,

$$S \equiv \frac{1}{M}\frac{\partial M}{\partial \ln t}\bigg|_{t=\tau} = \frac{-1}{(U/k_B T)-\ln(\tau/t_0)} , \tag{4.37}$$

which is appropriate as long as S is small, i.e., when

$$U/k_B T \geq \ln(\tau/t_0) \approx 30 , \tag{4.38}$$

where we have used the normalization time $\tau = 10$ min. Comparison of this criterion with Eq. (4.36) shows it is equivalent to the requirement $\tau > t_{cr}$. In other words, when S is small Eq. (4.27) is appropriate and we are in the long-time regime; when $S \geq 1/30$, Eq. (4.34) is the right choice.

The vortex-glass and collective-creep theories both offer different predictions for the value of μ: Feigel'man *et al.*[44] suggest $\mu = \frac{7}{9}$ for long-length scales, while the scaling approach of Nattermann[46] finds $\mu = \frac{1}{2}$. On the other hand, Dekker, Eidelloth, and Koch[45] argue that their low-current value of $\mu = 0.19 \pm 0.05$ supports a vortex-glass picture. In any event, both approaches suggest $0 < \mu \leq 1$. In Fig. 6, the plot of normalized logarithmic decay rate vs temperature, we see we are clearly in the long-time regime of Eq. (4.27) for all but the highest temperatures; however, $1/\mu$ vs T shown for the 500-G data in Fig. 11 shows $\mu \gg 1$ at low temperatures, inconsistent with both the collective-creep and vortex-glass pictures.

Furthermore, FFH argue that Eq. (4.34) implies the logarithmic decay rate vs temperature (as in Fig. 6) should be nonmonotonic for a vortex glass; and Malozemoff and Fisher[47] identify an apparently-universal non-monotonicity in the normalized logarithmic decay-vs-temperature data of several Y-Ba-Cu-O samples, and then suggest that this is a natural result of the vortex-glass picture. But this nonmonotonicity is not seen in our Nb samples. Figure 6 shows the normalized logarithmic decay rate increases *monotonically* with temperature for all fields, in contrast to the vortex-glass prediction.

V. VORTEX LATTICE MELTING

One common criterion for melting of a generic lattice is due to Lindemann.[48] His criterion identifies T_M, the melting temperature, as the temperature where the amplitude of the thermal fluctuations $\langle U^2 \rangle$ is equal to some fraction (typically 0.1) of the lattice spacing. Abrikosov vortex lattice melting was discussed in detail by Fisher.[20] He considered a two-dimensional system where the film thickness d was much less than the magnetic penetration depth λ. He found that the two-dimensional shear modulus $c_{66}d$ was so small the thermal fluctuations of the vortices from their equilibrium positions were large enough to melt the lattice at a temperature $T_M < T_c$. Nelson[49] made a calculation of $\langle U^2 \rangle$ for a bulk superconductor that was valid in the local elastic limit; while Moore[50] made an extension of earlier work on a distorted vortex lattice[51] and found a value of $\langle U^2 \rangle$ that was larger than Nelson's result. Meanwhile, Brandt's early work[52] on the elastic moduli of bulk, isotropic superconductors highlighted the importance of including nonlocal effects (i.e., the finite wave-vector dependence of the elastic moduli), especially when the Ginzburg-Landau parameter κ is large. In a more recent paper[53] he showed that Nelson's and Moore's results follow in a natural way from approximations to the detailed treatment, which includes the nonlocal elastic response of the vortex lattice. He used a Lindemann criterion to examine melting in bulk, isotropic superconductors. Houghton, Pelcovits, and Sudbø[19] performed a similar calculation which partially accounts for the anisotropy[53] of a uniaxially anisotropic material. Their melting line is given by

$$\frac{t_M}{\sqrt{1-t_M}}\frac{\sqrt{b}}{1-b}\left[\frac{4(\sqrt{2}-1)}{\sqrt{1-b}}+1\right]=\alpha , \tag{5.1}$$

where α, the degree of susceptibility to thermal motion, is given by

$$\alpha = 2\times 10^5 \left[\frac{c}{\kappa}\right]^2 \left[\frac{H_{c2}(0)}{T_c^2}\frac{M}{M_z}\right]^{1/2} . \tag{5.2}$$

Here $t_m = T_m/T_c(0)$, $b = H/H_{c2}(T)$, $H_{c2}(T) = H_{c2}(0)[1-T/T_c(0)]$, $\kappa \cong \lambda/\xi$ is the Ginzburg-Landau parameter, and M/M_z is the ratio of the in-plane and out-of-plane effective masses. The Lindemann criterion for melting is governed by the parameter c, which is the ratio of the mean-square thermal displacement of the vor-

tices from their equilibrium positions to the vortex lattice spacing. Suenaga *et al.*[25] have found good agreement between Eq. (5.1) and measurements on Nb_3Sn and Tb-Ti magnet wire, but were unable to make a meaningful comparison in the case of Nb because the difference between T_c and T^* had become too small.

The zero-field transition temperature $T_c(0)=9.11$ K and the zero-temperature upper critical field $H_{c2}(0)=15\,200$ G were determined by fitting the equation $H_{c2}(T)=H_{c2}(0)[1-T/T_c(0)]$ to the $H_{c2}(T)$ data shown in Fig. 2. The solid line in Fig. 2 is a single-parameter fit of Eq. (5.1) to the irreversibility line; the short-dashed line is the previously discussed $\frac{3}{2}$ power-law prediction from the depinning theory of Yeshuran and Malozemoff.[4] It is clear upon careful examination that the melting line provides the better fit, particularly in the lower-field and higher-temperature region.

Since $M/M_z=1$ for an isotropic superconductor, we can determine an upper bound for the Lindemann number c using the upper bound for κ of 10.8 determined in Sec. II. Combining κ with the curve-fit value for the parameter α gives the upper bound $c=0.04$ for our Nb sample. This is somewhat smaller than the values determined by Suenaga *et al.*[25] (For Nb_3Sn and Nb-Ti magnet wire, Suenaga found c to be 0.065 and 0.1, respectively.) It is substantially smaller than the value $c=0.4$ determined by Houghton for a Bi-Sr-Ca-Cu-O sample.

This might not be unexpected, however: As Brandt indicated in Ref. 53, the thermal fluctuations of the vortices from their equilibrium *positions* is not the only possible mechanism that could lead to melting of the vortex lattice. He calculated the thermal fluctuations of the *shear strain* and, using Schmucker's criterion[54] for the shear stress required to deform a lattice plastically, concluded: "smaller values $c\approx\frac{1}{20}$ appear thus more realistic." In addition, he offered five rather technical reasons why c might be even smaller still.

Also, in recent Monte Carlo simulations[55] Ryu and coworkers used a Lawrence-Doniach model of stacked superconducting layers to calculate a melting line for Bi-Sr-Ca-Cu-O sample of Houghton *et al.* Their criterion for melting was based on the disappearance of the in-plane translational order monitored by the Fourier transform of the density-density correlation function at the first Bragg point. They then obtained the value of c corresponding to this criterion by computing the root-mean-square deviation of the vortices from their equilibrium positions, thus obtaining a field-dependent Lindemann criterion for melting. They found that c decreased with decreasing flux line density, and hence, field. It ranged from 0.45 to 0.1 as the field went from 10^6 to 10^2 G. More important than the specific value, however, is the *trend* of their results: As the field shifts downward and the flux line density decreases, the interlayer coupling becomes relatively stronger than the in-plane correlations yielding a very fragile three-dimensional lattice of straighter flux lines— *and a lower Lindemann criterion.* This suggests that the Lindemann criterion for isotropic Nb might indeed be much lower than the value found for the Bi-Sr-Ca-Cu-O sample, which would be consistent with our results.

VI. CONCLUSIONS

In conclusion, we have identified the irreversibility line in Nb with the vortex lattice melting line. Below the irreversibility line, the remanent magnetization was found to decay logarithmically in time—at a rate that was well described by a conventional, single-activation-energy flux-creep picture. The data are inconsistent with the depinning theory of Yeshuran and Malozemoff,[4] and the vortex-glass theory of Fisher, Fisher, and Huse,[14] but they agree well with the melting model of Houghton *et al.*[19] The resulting value of the Lindemann criterion is lower than has been seen in high-T_c materials, but this is consistent with both the predictions of Brandt[53] and recent Monte Carlo simulations of Ryu *et al.*[55]

ACKNOWLEDGMENTS

The authors would like to thank P. H. Kes for useful discussions and S. Doniach for calling their attention to the important results of Ref. 55. This work was supported by the Low Temperature Physics program of the NSF under Grant No. NSF/DMR-9001874.

[1]K. A. Müller, M. Takashige, and J. G. Bednorz, Phys. Rev. Lett. **58**, 1143 (1987).

[2]D. J. Bishop *et al.*, Science **255**, 165 (1992); E. H. Brandt, Physica C **195**, 1 (1992); Y. Xu and M. Suenaga, Phys. Rev. B **43**, 5516 (1991).

[3]M. Tuominen, A. M. Goldman, and M. L. Mecartney, Physica C **153-155**, 324 (1988).

[4]Y. Yeshuran and A. P. Malozemoff, Phys. Rev. Lett. **60**, 2202 (1988).

[5]M. Tinkham, Helv. Phys. Acta **61**, 443 (1988); M. Tinkham, Phys. Rev. Lett. **61**, 1658 (1988); M. Tinkham and C. J. Lobb, in *Physical Properties of the New Superconductors,* edited by H. Ehrenreich and D. Turnbull, Solid State Physics Vol. 42 (Academic, New York, 1989).

[6]C. W. Hagen and R. Griessen, Phys. Rev. Lett. **62**, 2857 (1989).

[7]M. Konczykowski, F. Rullier-Albenque, E. R. Yacoby, A. Shaulov, Y. Yeshuran, and P. Lejay, Phys. Rev. B **44**, 7167 (1991).

[8]L. Civale, A. D. Marwick, M. W. McElfresh, T. K. Worthington, A. P. Malozemoff, F. H. Holtzberg, J. R. Thompson, and M. A. Kirk, Phys. Rev. Lett. **65**, 1164 (1990).

[9]R. Wördenweber, Phys. Rev. B **46**, 3076 (1992); P. H. Kes and J. van den Berg, in *Studies of High Temperature Superconductors,* edited by A. Narlikar (Nova Science, New York, 1990).

[10]M. P. A. Fisher, Phys. Rev. Lett. **62**, 1415 (1989).

[11]A. I. Larkin and Y. N. Ovchinnikov, J. Low Temp. Phys. **34**, 409 (1979).

[12]R. H. Koch, V. Foglietti, W. J. Gallagher, G. Koren, A. Gupta, and M. P. A. Fisher, Phys. Rev. Lett. **63**, 1511 (1989).

[13]P. L. Gammel, L. F. Schneemeyer, and D. J. Bishop, Phys.

Rev. Lett. **66**, 953 (1991).
[14]D. S. Fisher, M. P. A. Fisher, and D. A. Huse, Phys. Rev. B **43**, 130 (1991).
[15]C. A. Murray, P. L. Gammel, D. J. Bishop, D. B. Mitzi, and A. Kapitulnik, Phys. Rev. Lett. **64**, 2312 (1990).
[16]C. Rossel, Y. Maeno, and I. Morgenstern, Phys. Rev. Lett. **62**, 681 (1989).
[17]M. Charalambous, J. Chaussy, and P. Lejay, Phys. Rev. B **45**, 45 (1992).
[18]R. E. Hetzel, A. Sudbø, and D. A. Huse, Phys. Rev. Lett. **69**, 518 (1992).
[19]A. Houghton, R. A. Pelcovits, and A. Sudbø, Phys. Rev. B **40**, 6763 (1989).
[20]D. S. Fisher, Phys. Rev. B **22**, 1190 (1980).
[21]D. E. Farrel, J. P. Rice, and D. M. Ginsberg, Phys. Rev. Lett. **67**, 1165 (1991); R. G. Beck, D. E. Farrel, J. P. Rice, D. M. Ginsberg, and V. G. Kogan, *ibid.* **68**, 1594 (1992).
[22]H. Safar, P. L. Gammel, D. A. Huse, D. J. Bishop, J. P. Rice, and D. M. Ginsberg, Phys. Rev. Lett. **69**, 824 (1992).
[23]W. K. Kwok, S. Fleshler, U. Welp, V. M. Vinokur, J. Downey, G. W. Crabtree, and N. M. Miller, Phys. Rev. Lett. **69**, 3370 (1992).
[24]P. L. Gammel, L. F. Schneemeyer, J. V. Wasczak, and D. J. Bishop, Phys. Rev. Lett. **61**, 1666 (1988).
[25]M. Suenaga, A. K. Ghosh, Y. Xu, and D. O. Welch, Phys. Rev. Lett. **66**, 1777 (1991).
[26]H. Drulis, Z. G. Xu, J. W. Brill, L. E. De Long, and J.-C. Hou, Phys. Rev. B **44**, 4731 (1991).
[27]C. J. van der Beek, Ph.D. thesis, Leiden University, 1992 (unpublished), pp. 106–108.
[28]G. M. Stollman, B. Dam, J. H. P. M. Emmen, and J. Pankert, Physica C **161**, 444 (1989).
[29]M. Suenaga, D. O. Welch, and R. Budhani, Supercond. Sci. Technol. **5**, 1 (1992).
[30]C. V. Tomy, R. Kumar, and A. K. Grover, Solid State Commun. **80**, 117 (1991).
[31]S. Ramakrishnan, R. Kumar, P. L. Paulose, A. K. Grover, and P. Chaddah, Phys. Rev. B **44**, 9514 (1991).
[32]H. Obara, S. Kosaka, Y. Yokoyama, M. Umeda, and Y. Kimura, Phys. Rev. B **44**, 4532 (1991).
[33]Z. J. Huang, H. H. Fang, Y. Y. Xue, P. H. Hor, and C. W. Chu, Physica C **180**, 331 (1991).
[34]C. W. Hagen and R. Griessen, Phys. Rev. Lett. **65**, 1284 (1990).
[35]C. P. Bean, Phys. Rev. Lett. **8**, 250 (1962).
[36]P. W. Anderson, Phys. Rev. Lett. **9**, 309 (1962); Y. B. Kim, Rev. Mod. Phys. **36**, 39 (1964).
[37]M. Tinkham, in *Introduction to Superconductivity* (Krieger, Malabar, FL, 1980), Chap. 5.
[38]A. M. Campbell and J. E. Evetts, Adv. Phys. **21**, 199 (1972).
[39]J. R. L. de Almeida and D. J. Thouless, J. Phys. A **11**, 983 (1978).
[40]K. H. Lee and D. Stroud, Phys. Rev. B **44**, 9780 (1991).
[41]S. N. Coppersmith, M. Inui, and P. B. Littlewood, Phys. Rev. Lett. **64**, 2585 (1990).
[42]R. H. Koch, V. Foglietti, and M. P. A. Fisher, Phys. Rev. Lett. **64**, 2586 (1990).
[43]C. J. van der Beek, Ph.D. thesis, Leiden University, 1992 (unpublished), p. 106, Fig. 5.7.
[44]M. V. Feigel'man, V. B. Geshkenbein, A. I. Larkin, and V. M. Vinokur, Phys. Rev. Lett. **63**, 2303 (1989).
[45]C. Dekker, W. Eidelloth, and R. W. Koch, Phys. Rev. Lett. **68**, 3347 (1992).
[46]T. Nattermann, Phys. Rev. Lett. **64**, 2454 (1990).
[47]A. P. Malozemoff and M. P. A. Fisher, Phys. Rev. B **42**, 6784 (1990).
[48]F. Lindemann, Phys. Z **11**, 69 (1910).
[49]D. R. Nelson, Phys. Rev. Lett. **60**, 1973 (1988); D. R. Nelson and H. S. Seung, Phys. Rev. B **39**, 9174 (1989).
[50]M. A. Moore, Phys. Rev. B **39**, 136 (1989).
[51]G. Eilenberger, Phys. Rev. **164**, 628 (1967).
[52]E. H. Brandt, J. Low Temp. Phys. **26**, 709 (1977); **26**, 735 (1977); **28**, 263 (1977); **28**, 291 (1977).
[53]E. H. Brandt, Phys. Rev. Lett. **63**, 1106 (1989).
[54]R. Schmucker, Philos. Mag. **35**, 431 (1977).
[55]S. Ryu, S. Doniach, G. Deutscher, and A. Kapitulnik, Phys. Rev. Lett. **68**, 710 (1992).